

# Optimization of Conductive Filament of Oxide-based RRAM for Low Operation Current by Stochastic Simulation

P. Huang, Y.X. Deng, B. Gao, B. Chen, F.F. Zhang, D. Yu, L.F. Liu, G. Du, J.F. Kang\*, and X.Y. Liu\*

Institute of Microelectronics, Peking University, Beijing 100871, China,

\*E-mail: kangjf@pku.edu.cn, xyliu@ime.pku.edu.cn

## 1. Introduction

Resistive-switching random access memory (RRAM) based on metal oxides has attracted considerable interests for next generation Non-Volatile Memory devices due to the excellent scalability, high density and memory performance, and compatibility with the CMOS process [1]. Despite some progresses [1, 2], there are still many challenges for commercial utilization of metal oxide RRAM such as high Reset current [1]. The Forming operation current will directly decide the subsequent Reset current [3] and the current overshoot during the Forming process will cause a larger Reset current [4]. Therefore, a study of the Forming process to suppress the current overshoot is imperative. It is widely accepted that the resistive switching in metal oxide RRAM is attributed to the formation and dissolution of conductive filament (CF) consisting of oxygen vacancies ( $V_O$ ) [5-7]. In this paper, we report and demonstrate a stochastic simulator to self-consistently simulate the evolution of CF in the Forming process. Based on the stochastic simulator, the optimization approach of CF by controlling of CF evolution to suppress the current overshoot to achieve low operation current is addressed. The achieved results are helpful for low current RRAM design and application.

## 2. Model and Simulation

**Fig.1** schematically illustrates the resistive switching mechanism correlated with the Forming process in metal oxide RRAM [6], which can be depicted by the equations as shown in **Table I**. Under the external bias,  $V_O$  generation is a random process and the generation probability ( $P_a$ ) is expressed as **Eq. (1)** [6]. And the probability of  $O^{2-}$  hopping to the neighbored interstitial sites ( $P_h$ ) is controlled by **Eq. (2)** [7]. When  $O^{2-}$  is located at the neighbor of  $V_O$ , the recombination occurs with the lifetime  $t_0$  ( $10^{-6}$  s) [7]. The process of  $O^{2-}$  absorbed and released by electrode are the same as the  $O^{2-}$  hopping, except that the barrier changes to  $E_i$  (1.0eV) [7]. Stochastic method is used to simulate the above microscopic processes. To simulate the above mentioned microscopic processes self-consistently and efficiently, a resistor network based on the percolation theory [8, 9] is introduced. For the simplification, we assume the IV-characteristics between two  $V_O$ ,  $V_O$  and electrode are the same and can be described as **Eq. (3)**, while the other resistance is modeled as **Eq. (4)**. The potential and current can be solved by the Kirchhoff law and the located temperature can be given by the Fourier heat-flow equation (**Eq. (5)**) at the time after each microscopic process which ensures our simulation is self-consistent. The flowchart of the stochastic simulator is shown in **Fig.2**.

## 3. Results and Discussion

Firstly, the Forming process of oxide-based RRAM is simulated and compared with the measured data of TiN/HfO<sub>x</sub>/Pt RRAM, as reported in our previous work [10]. **Fig.3** shows  $V_O$  evolution during a Forming process. A fine CF is firstly formed to connect the two electrodes. Then it rapidly develops into a strong conical shape of CF under external bias, consistent with previous conjecture based on the experimental data [5]. **Fig.4** plots the simulated and measured IV-curves. A current abrupt behavior is reproduced and verified by the measured data. **Fig.5** shows the comparison of the simulated  $V_{Forming}$  values with measured data at different cell thicknesses and temperatures. **Fig.6** shows the cumulative probability distribution of the  $V_{Forming}$  values simulated and measured on 40 RRAM devices. These good agreements between simulations and measured data demonstrate the validity and accuracy of the developed stochastic simulator for the Forming process.

The characteristics of CF evolution under various switching parameters are explored by the developed simulator. As shown in **Fig.4**, compliance current is used to prevent an irreversible thermodynamic dielectric breakdown. However, the practical measurement equipment or the intrinsic parasitic effect has a delay time which leads to current overshoot over the desired limit and results in a high Reset current. **Fig.7** shows the CF shapes comparison between the case without and with 0.2ns delay time. It reveals that current overshoot will lead to a stronger CF. The current overshoot is decided by two factors: the delay time and the CF expanding rate. Here, we focus on the issue how to control the CF expanding rate. We evaluate that the CF expanding rate depends on the time interval between two different current values during the CF expanding process, in which longer time interval means slower CF expanding rate. **Fig.8~11** shows the interval time with different sweep rate, ambient temperature, doping concentration and pre-exist  $V_O$  concentration. The doping element considered in this work will reduce  $E_a$  to 1.0 eV. It reveals that low sweep rate, high ambient temperature, high doping concentration and high pre-exist  $V_O$  concentration are helpful to reduce the CF expanding rate, consequently the Reset current.

## 4. Conclusions

We report and demonstrate a stochastic simulator to self-consistently simulate the evolution of CF during the Forming process. Our simulation results reveal that low sweep rate, high ambient temperature, high doping concentration and high pre-exist  $V_O$  concentration are beneficial to the controlled CF evolution rate and the suppressed current overshoot effect, which is critical to achieve a low Reset current and low operation power.

## Acknowledgement

This work is supported by the National Fundamental Basic Research Program of China (Grant No 2011CBA00600).

## References

[1] Y.S. Chen et al, IEDM2011, p717. [2] I. G. Baek et al, IEDM 2011, p737. [3] Y.S.Chen et al, VLSI-TSA2011. [4] D.C.Gilmer et

al, IMW2011. [5] G. Bersuker et al, IEDM2010, p.456. [6] B. Gao et al, IEDM2011, p.417. [7] S.Yu et al, EDL, 31, p1455 (2010). [8] S.C. Chae et al, Adv. Mater., 20, p1154 (2008). [9] Dietrich Stauffer et al, Introduction to percolation theory, 2003. [10] B.Chen et al, EDL, 32, p282 (2011). [11] Xuhui Luo et al, PRB, 80,134119 (2009). [12] S.-M. Lee et al, PRB, 52, p253 (1995).

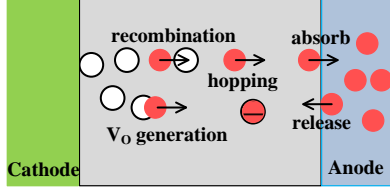


**Fig.1** Schematically physical mechanism of the Forming process in metal oxide RRAM. V<sub>O</sub> CF is formed due to the ionization of O<sup>2-</sup> from the lattice sites. The distance between two oxygen sites is 0.5nm. The simulation region is 10nm×50nm.

**Table I** Correlation equations of resistive switching behaviors with Forming process.

$$\text{Eq. (1)} P_a = ft \exp(-(E_a - \Delta\phi_1) / k_B T_{loc})$$

$$\text{Eq. (2)} P_h = ft \exp(-(E_h - \Delta\phi_2) / k_B T_{loc})$$

f: vibration frequency~10<sup>13</sup> Hz [6], E<sub>a</sub>: activation energy of V<sub>O</sub>~1.2eV [6], E<sub>h</sub>: hopping barrier~0.9eV [7].

$$\text{Eq. (3)} I = U / R_1 \quad \text{Eq.(4)} I = \sinh(\alpha U) / R_2$$

$$R_1 \sim 10^6 \Omega \quad R_2 \sim 4.5 \times 10^{13} \Omega \quad \alpha \sim 37$$

$$\text{Eq. (5)} C \frac{\partial T}{\partial t} = \nabla(k \cdot \nabla T) + Q$$

C: thermal capacity of metal oxide~6×10<sup>6</sup> J/m<sup>3</sup>K [11]; k: thermal conductivity of metal oxide~5 W/mK [12].

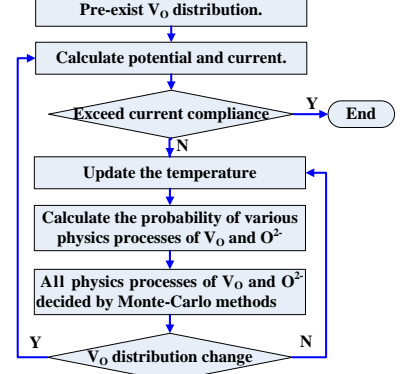


**Fig.2** Schematic of the simulation flowchart used in this study.

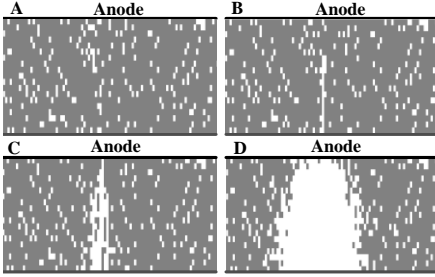


**Fig.3** V<sub>O</sub> evolution during Forming process. The white dots represent the V<sub>O</sub>. A conical shape CF between two electrodes is formed during a Forming process, excellent consistency is observed.

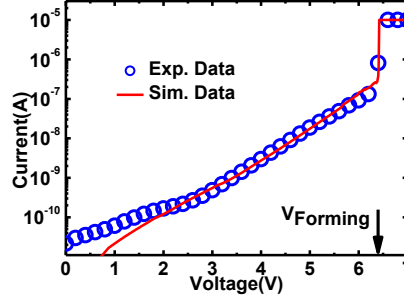


**Fig.4** Simulated and measured IV-curves during a Forming process, excellent consistency is observed.

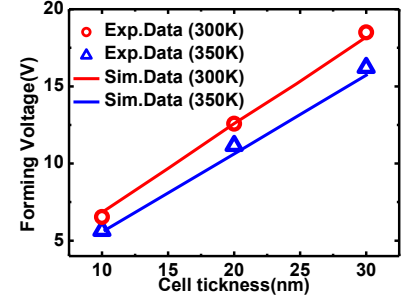


**Fig.5** Comparison between simulated and measured Forming voltage with different thickness under different temperature.

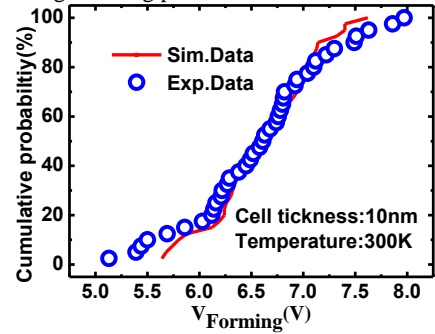


**Fig.6** Simulated V<sub>Forming</sub> values cumulative distribution, which is consistent with the measured data.

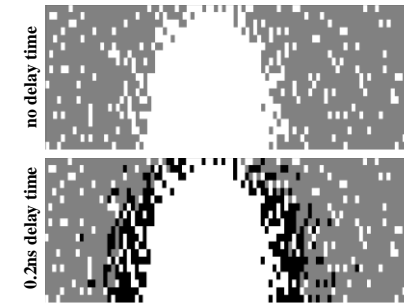


**Fig. 7** Simulated CF shapes without delay time and with 0.2ns delay time. The black dots represent the new generation V<sub>O</sub> in the delay time.

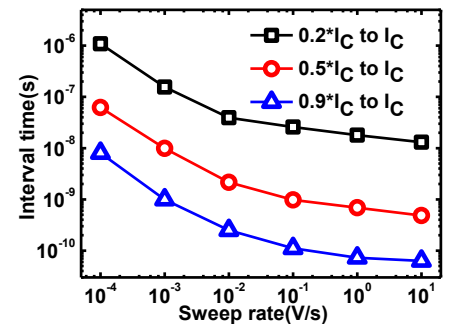


**Fig.8** Simulated interval time between two different current values during the CF expanding process with different sweep rate.

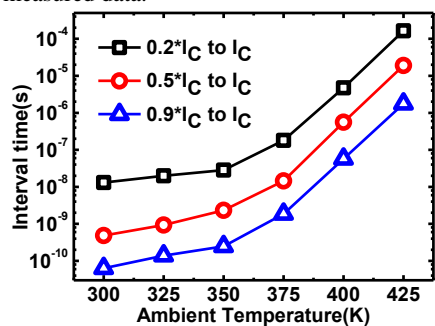


**Fig.9** Simulated interval time between two different current values during the CF expanding process under different temperature.

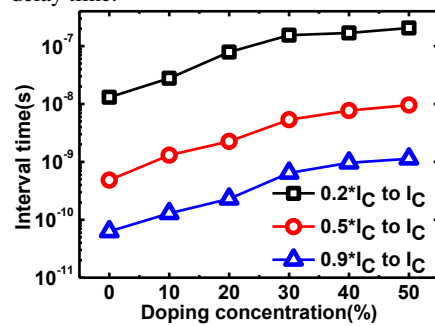


**Fig.10** Simulated interval time between two different current values with different doping concentration.

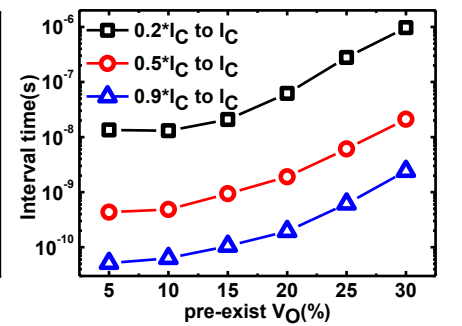


**Fig.11** Simulated interval time between two different current values during the CF expanding process with different pre-exist V<sub>O</sub>.